Induced pluripotent stem cell model recapitulates pathologic hallmarks of Gaucher disease

Leelamma M. Panicker[a], Diana Miller[a], Tea Soon Park[b,c], Brijesh Patel[a], Judi L. Azevedo[a], Ola Awad[a], M. Athar Masood[d], Timothy D. Veenstra[d], Ehud Goldin[e], Barbara K. Stubblefield[e], Nahid Tayebi[e], Swamy K. Polumuri[a], Stefanie N. Vogel[a], Ellen Sidransky[e], Elias T. Zambidis[b,c], and Ricardo A. Feldman[a,1]

[a]Department of Microbiology and Immunology, University of Maryland School of Medicine, Baltimore, MD 21201; [b]Institute for Cell Engineering and [c]Sidney Kimmel Comprehensive Cancer Center at The Johns Hopkins University School of Medicine, Baltimore, MD 21205, [d]Laboratory of Proteomics and Analytical Technologies, SAIC-Frederick, Inc., Frederick National Laboratory for Cancer Research, Frederick, MD 21702; and [e]Medical Genetics Branch, National Human Genome Research Institute, National Institutes of Health, Bethesda, MD 20892

Edited by George Q. Daley, Children's Hospital Boston, Boston, MA, and accepted by the Editorial Board September 13, 2012 (received for review May 10, 2012)

Gaucher disease (GD) is an autosomal recessive disorder caused by mutations in the acid β-glucocerebrosidase gene. To model GD, we generated human induced pluripotent stem cells (hiPSC), by reprogramming skin fibroblasts from patients with type 1 (N370S/N370S), type 2 (L444P/Rec*NciI*), and type 3 (L444P/L444P) GD. Pluripotency was demonstrated by the ability of GD hiPSC to differentiate to all three germ layers and to form teratomas in vivo. GD hiPSC differentiated efficiently to the cell types most affected in GD, i.e., macrophages and neuronal cells. GD hiPSC-macrophages expressed macrophage-specific markers, were phagocytic, and were capable of releasing inflammatory mediators in response to LPS. Moreover, GD hiPSC-macrophages recapitulated the phenotypic hallmarks of the disease. They exhibited low glucocerebrosidase (GC) enzymatic activity and accumulated sphingolipids, and their lysosomal functions were severely compromised. GD hiPSC-macrophages had a defect in their ability to clear phagocytosed RBC, a phenotype of tissue-infiltrating GD macrophages. The kinetics of RBC clearance by types 1, 2, and 3 GD hiPSC-macrophages correlated with the severity of the mutations. Incubation with recombinant GC completely reversed the delay in RBC clearance from all three types of GD hiPSC-macrophages, indicating that their functional defects were indeed caused by GC deficiency. However, treatment of induced macrophages with the chaperone isofagomine restored phagocytosed RBC clearance only partially, regardless of genotype. These findings are consistent with the known clinical efficacies of recombinant GC and isofagomine. We conclude that cell types derived from GD hiPSC can effectively recapitulate pathologic hallmarks of the disease.

Gaucher model | Gaucher macrophages | lipid storage disease | glucosylsphingolipids | erythrophagocytosis

Gaucher disease (GD) is the most frequently inherited lipid storage disease; it primarily affects Ashkenazi Jews, where carrier frequency is 1 in 18 and disease incidence is 1 in 1,000, compared with 1 in 50,000 in the general population (1). GD is caused by mutations in the acid β-glucocerebrosidase (*GBA*) gene. Type 1 GD is the most common and mildest form of the disease and affects primarily reticuloendothelial cells. The reduced glucocerebrosidase (GC) activity in phagocytic cells results in lysosomal accumulation of glucosylceramide (GlcCer) and other sphingolipids, derived mostly from the breakdown of ingested red and white blood cell membranes (2, 3). Patients affected with type 1 GD exhibit hepatosplenomegaly, hematologic abnormalities, and bone disease (1, 4). Type 2 GD is an acute form of the disease and is usually fatal before 2 y of age. Type 3 GD tends to have a later onset and is subacute. In patients who have type 2 and 3 GD, in addition to hematologic and visceral manifestations, there is brain involvement of unclear etiology. Patients with GD present with heterogeneous symptoms, even among patients with the same *GBA* mutations. This heterogeneity suggests that genetic background and environmental factors may also influence the severity of the disease (5).

One obstacle to modeling GD is that the disease-affected cell types are not easily available. Human macrophages can be obtained from peripheral blood, but they are difficult to expand in culture, and patient-derived neuronal cell types are even more difficult to procure. GD fibroblasts have been widely used for studying the disease and for therapeutic development, but these cells are nonphagocytic and do not release the inflammatory mediators and hydrolases believed to play a role in GD pathology. Additionally, fibroblasts are of limited utility for studying the underlying causes of neuronopathic GD. These limitations may be overcome by reprogramming patient-derived cells into human induced pluripotent stems cells (hiPSC), as first shown by Yamanaka and coworkers (6, 7). hiPSC have been derived from patients affected by a variety of diseases (8–11), including long QT syndrome (12, 13), familial dysautonomia (14), and Alzheimer's disease (15), and important aspects of the disease phenotype have been recapitulated in the relevant hiPSC-derived cell types (16).

In this study we report the development of hiPSC derived from patients harboring the most frequent mutations associated with development of types 1, 2, and 3 GD. GD hiPSC were differentiated to macrophages and neuronal cells that were found to accumulate sphingolipids in a pathologic manner. In mutant macrophages, GC deficiency resulted in ineffective clearance of phagocytosed RBC, which is a classic hallmark of the disease (17, 18). Moreover, the extent of the functional defect exhibited by types 1, 2, and 3 GD hiPSC-macrophages in vitro reflected the severity of the mutation. Our results suggest that this hiPSC model recapitulates the phenotypic and pathological variants of the disease, and can be a valuable tool for understanding molecular mechanisms and developing therapeutic approaches for GD.

Results

Generation of GD hiPSC. GD fibroblasts from patients with types 1, 2, and 3 GD were reprogrammed by expression of SOX2, OCT4, KLF4, and MYC after infection with the STEMCCA vector, and initial hiPSC colony selection was based on morphologic resemblance to human embryonic stem cell (hESC) colonies (Fig. S1*A*). As shown in Fig. 1*A*, L444P/Rec*NciI* GD hiPSC expressed typical pluripotency surface markers, including SSEA-3, SSEA-4, TRA-1–60, and TRA-1–81. They also expressed undifferentiated

Author contributions: L.M.P., D.M., T.S.P., J.L.A., O.A., and R.A.F. designed research; L.M.P., D.M., T.S.P., B.P., J.L.A., O.A., M.A.M., T.D.V., E.G., N.T., and R.A.F. performed research; T.S.P., M.A.M., T.D.V., E.G., B.K.S., S.K.P., S.N.V., E.S., and E.T.Z. contributed new reagents/analytic tools; L.M.P., D.M., T.S.P., B.P., J.L.A., O.A., M.A.M., T.D.V., E.G., N.T., S.N.V., E.T.Z., and R.A.F. analyzed data; and L.M.P. and R.A.F. wrote the paper.

The authors declare no conflict of interest.

This article is a PNAS Direct Submission. G.Q.D. is a guest editor invited by the Editorial Board.

Freely available online through the PNAS open access option.

[1]To whom correspondence should be addressed. E-mail: rfeldman@umaryland.edu.

This article contains supporting information online at www.pnas.org/lookup/suppl/doi:10.1073/pnas.1207889109/-/DCSupplemental.

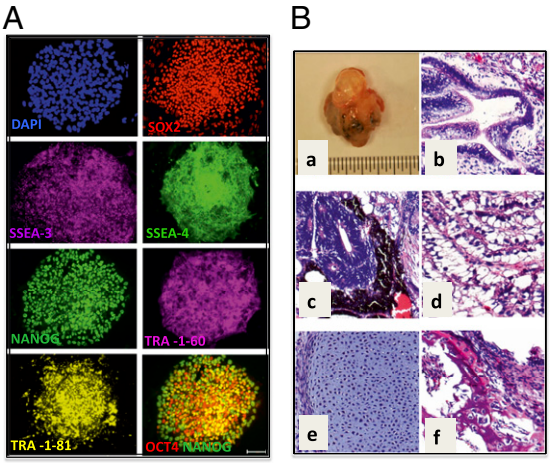

Fig. 1. Generation and characterization of L444P/Rec*NciI* (type 2) GD hiPSC. (*A*) Staining of GD hiPSC with antibodies to the stem cell and pluripotency markers SOX2, SSEA-3, SSEA-4, NANOG, TRA-1–60 TRA-1–81, and OCT4. (Scale bar, 100 μm.) (*B*) (*a*) GD hiPSC cells gave rise to benign cystic teratomas in NOG-SCID mice. (*b–f*) H&E staining of teratoma cells from the three germ layers. (*b*) Glandular structure. (*c*) Pigmented neural epithelium and rosettes. (*d*) Intestinal epithelium. (e) Cartilage. (*f*) Bone. (Magnification: 20×.)

ES cell markers such as NANOG, SOX2, and OCT4 but did not express SSEA-1, a marker for differentiation in human cells. Marker analysis was done with five independently derived GD hiPSC lines, all with similar results. Quantitative analysis of marker expression by flow cytometry confirmed that the majority of GD hiPSC expressed these pluripotency markers (Fig. S1*B*). Similar analysis of independently derived colonies of N370S/N370S (type 1) and L444P/L444P (type 3) GD hiPSC showed that they all expressed pluripotency and undifferentiated ES cell markers (see Fig. S4 *A* and *B*). Karyotypic analysis of GD hiPSC lines indicated a normal complement of chromosomes (Fig. S2*A*).

Pluripotency of GD hiPSC. Pluripotency of GD hiPSC was demonstrated through their ability to give rise to all three germ layers in vitro and in vivo. After 15 d in differentiation culture, GD embryoid bodies (EBs) from type 2 L444P/Rec*NciI* hiPSC stained positive for the ectodermal markers neuronal-specific tubulin (Tuj1) and microtubule-associated protein 2 (MAP2) (Fig. S2*B*). These EBs also were positive for the mesodermal marker brachyury and the endodermal marker GATA4. To assay pluripotency in vivo, type 2 GD hiPSC were injected s.c. into NOG/SCID mice. Teratomas arose within 6–8 wk of injection from all three GD hiPSC lines tested (Fig. 1 *B*, *a*). Histopathological analysis showed the presence of multiple cell lineages within the benign tumors, representative of all three germ layers, including glandular, intestinal, neuronal, bone, and cartilage structures from the type 2 hiPSC (Fig. 1 *B*, *b–f*). The type 1 (N370S/N370S) and type 3 (L444P/L444P) hiPSC also were pluripotent, as assessed in vitro and by teratoma formation in NOG/SCID mice in vivo (see Fig. S4 *C* and *D*).

Directed Differentiation of GD hiPSC to Monocyte/Macrophages. GD hiPSC cultured in suspension as EBs for a week differentiated into hematopoietic cells that stained positive for CD11b and CD14 (Fig. S3*B*). From around day 15 onwards, round monocyte-like cells arose from the middle of the flattened EBs and floated in the culture medium. Fig. S3*A* shows different stages of an EB culture that led to monocyte production. Monocytes harvested from the culture supernatant showed a single uniform population, and more than 95% of both GD hiPSC- and control hiPSC-monocytes expressed CD14 (Fig. 2*A* and Fig. S2*C*, respectively). Under optimal conditions, monocyte-producing factories yielded more than one million cells per four or five EBs every 4–5 d. The cultures produced monocytes for more than 3 mo, but yields diminished with time.

To generate GD macrophages, GD hiPSC-monocytes were plated onto adherent plates in the presence of M-CSF. After 3 d, May–Grünwald–Giemsa staining showed the presence of cells with the typical appearance of macrophages with round or spread-out morphologies (Fig. 2 *C*, *a–c*). These cells expressed typical markers of macrophage differentiation including CD14, CD163, and CD68 (Fig. 2 *B*, *a–c*). Similar results were obtained by directed differentiation of control hiPSC (Figs. S2 *D*, *a–c* and S3*C*) and H9/hESC (Fig. S3*D*), as well as N370S/N370S (Fig. S4*E*) and L444P/L444P hiPSC (Fig. S4*F*).

GD hiPSC-Macrophages Phagocyte Opsonized RBC. Tissue macrophages have multiple functions, including the removal of aged and damaged red and white blood cells from circulation. To determine whether GD macrophages were able to carry out phagocytosis of RBC, L444P/Rec*NciI* type 2 GD macrophages were incubated with opsonized RBC for 2 h at 37 °C. As shown in Fig. 2 *D*, *a* and *b* (live-cell images) and Fig. 2 *D*, *d* and *e* (May–Grünwald–Giemsa staining), the GD hiPSC-macrophages had high phagocytic activity, and the majority of cells were able to ingest 15–50 RBC. This activity also was seen in macrophages derived from two other type 2 GD hiPSC lines we tested. RBC ingestion by GD hiPSC-macrophages was similar to that in control hiPSC- and hESC-macrophages (Fig. S3 *E*, *a* and *F*, *a*), suggesting that GC deficiency did not alter the erythrophagocytic activity of the mutant macrophages. Type 1 N370S/N370S and type 3 L444P/L444P hiPSC-macrophages were able to phagocytose opsonized RBC with efficiency similar to that of type 2 L444P/Rec*NciI* macrophages.

GD hiPSC-Macrophage Activation in Response to LPS. To determine whether GD hiPSC-macrophages would respond to bacterial products, we treated control and GD hiPSC-macrophages with the bacterial endotoxin LPS (19). As shown in Fig. 2*E*, 2-h treatment of control and type 2 GD hiPSC-macrophages with LPS induced the production of high levels of TNF-α, IL-10, IL-12 p35, and IL-12 p40 mRNA. The level of induction of the inflammatory cytokine TNF-α was significantly higher in GD hiPSC- than in control hiPSC-macrophages. Future studies should clarify whether GC deficiency sensitizes GD macrophages toward inflammatory responses, as suggested by clinical observations (3). Taken together, the ability of GD hiPSC-derived macrophages to phagocyte RBC and to respond to LPS strongly suggests that they have the functional properties of mature macrophages.

GD hiPSC-Macrophages Have Reduced GC Activity and Accumulate Sphingolipids. As shown in Fig. 3*A*, the GC enzymatic activity in N370S/N370S, L444P/L444P, and L444P/Rec*NciI* hiPSC-macrophages was less than 5% of that in hiPSC-macrophage controls from a healthy donor, even though the mutant proteins in the three types of GD macrophages were still expressed at about 50% of control levels (Fig. 3*A*). In patients with GD, cells of the reticuloendothelial system display characteristic lipid accumulation because of the inability to digest GlcCer derived from normal metabolism and from the phagocytosis of red and white blood cells. This accumulation leads to the appearance of lipid-engorged Gaucher macrophages (20), in which remnants of RBC are often seen (17, 18, 21, 22). To assess whether GD hiPSC-macrophages would recapitulate the lipid accumulation seen in macrophages of patients with GD, we carried out immunofluorescence analysis using an antibody specific to GlcCer and HPLC-MS/MS. As shown in Fig. 3 *B*, *a* and *b*, mutant hiPSC-macrophages had elevated levels of GlcCer as compared with control cells (Fig. 3 *B*, *c* and *d*). HPLC-MS/MS analysis showed that types 2 and 3 GD hiPSC-macrophages had a 90-fold increase in glucosylsphingosine as compared with control hiPSC-macrophages, whereas type 1 GD macrophages exhibited a lower, but still very significant, 28-fold increase of this lipid (Fig. 3*C* and Fig. S5). These results show that

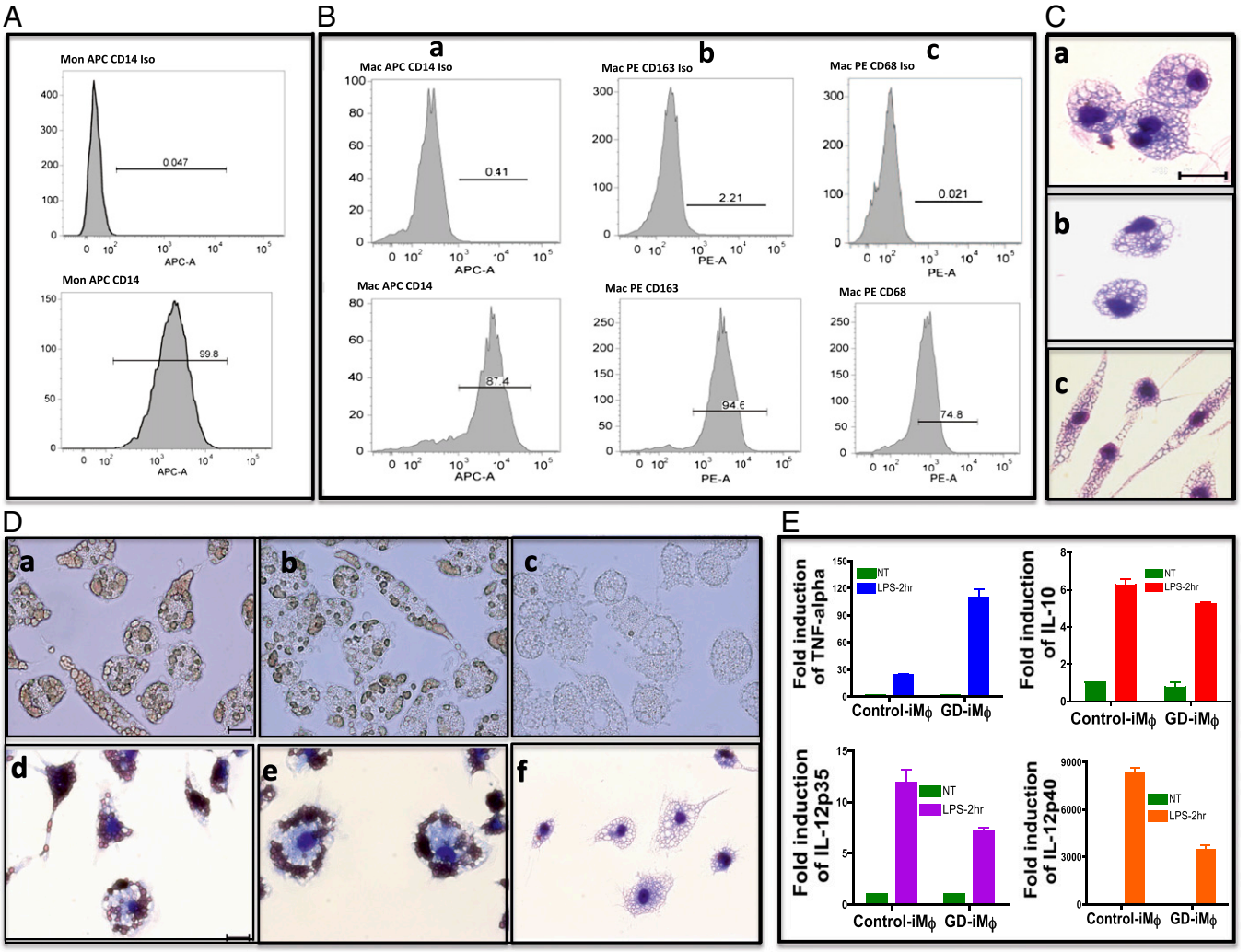

Fig. 2. Directed differentiation of type 2 GD hiPSC to monocyte/macrophages. (*A* and *B*) FACS analysis of L444P/Rec*NciI* hiPSC-monocyte/macrophages. Histograms show the percentage of cells stained with antibodies to specific markers (*Lower*) and isotype controls (*Upper*). (*A*) CD14 expression in GD hiPSC-monocytes. (*B*) Expression of CD14 (*a*), CD163 (*b*), and CD68 (*c*) in GD hiPSC-macrophages. (*C*) May–Grünwald–Giemsa staining showing the appearance of GD hiPSC-macrophages with different morphologies (*a*–*c*). (Scale bar, 20 μm.) (*D*) (*a*, *b*, *d*, and *e*) Phagocytosis of opsonized RBC by GD hiPSC-macrophages. (*c* and *f*) Non-opsonized RBC control. (*a*–*c*) Live-cell images of GD hiPSC-macrophages. (*d*–*f*), May–Grünwald–Giemsa staining of GD hiPSC-macrophages. (Scale bars, 20 μm.) (*E*) RT-PCR analysis showing the induction of TNF-α, IL-10, IL-12p35, and IL-12p40 mRNA in response to LPS treatment. Numbers in the ordinates represent the fold-activation of corresponding cytokines compared with the nontreated condition. *P* values for fold-cytokine induction in GD hiPSC-macrophages compared with control hiPSC-macrophages are $P < 0.0138$ (TNF-α), $P < 0.1$ (IL-10), $P < 0.0698$ (IL-12p35), and $P < 0.009$ (IL-12p40).

the levels of GC activity in patient-derived hiPSC-macrophages were not sufficient to catabolize glucosylsphingolipids generated by normal metabolism in the mutant cells, even in case of the milder N370S mutant.

Impaired Clearance of RBC in GD hiPSC-Macrophages. When characterizing the phagocytic properties of type 2 GD hiPSC-macrophages, we noticed a significant delay in the clearance of ingested RBC by mutant macrophages compared to control macrophages, as determined by direct observation under the microscope. The internalized RBC were visible inside macrophages derived from both control and GD hiPSC-macrophages for a few hours after ingestion. However, we noticed that although ingested RBC were no longer visible in control hiPSC-macrophages after 24 h, remnants of RBC were visible in mutant macrophages even 3 d after erythrophagocytosis. To confirm these observations, we quantified the rate of clearance of phagocytosed RBC by GD hiPSC-macrophages. As shown in Fig. 3*D*, control hiPSC- and hESC-macrophages were able to clear most of the ingested RBC within 1 d. However, macrophages derived from three different L444P/Rec*NciI* hiPSC lines exhibited a significant delay in RBC clearance (Fig. 3*D*). Fig. 3*E* shows the presence of significant numbers of engulfed RBC in the L444P/Rec*NciI* type 2 macrophages (Fig. 3 *E*, *a* and *b*) compared with control macrophages (Fig. 3 *E*, *c* and *d*) 24 h after phagocytosis. L444P/L444P (type 3) and N370S/N370S (type 1) hiPSC-macrophages also exhibited impaired RBC clearance, and the extent of the delay in RBC clearance increased with the severity of the mutation (Fig. 3*F*). It is worth noting that the level of sphingolipid accumulation was very similar in type 2 L444P/Rec*NciI* and type 3 L444P/L444P hiPSC-macrophages (Fig. 3*C*), suggesting that the RBC clearance assay was better able to predict clinical subtype than measurement of sphingolipid accumulation.

Because the presence of RBC remnants is a key feature of macrophages that infiltrate bone marrow and other organs in patients with GD (17, 18, 21, 22), the GD hiPSC-macrophages we obtained recapitulate an important hallmark of the disease. This abnormal RBC clearance by mutant macrophages might be caused by blockage of the phagocytic pathway downstream of RBC uptake, because there were no quantitative differences in the

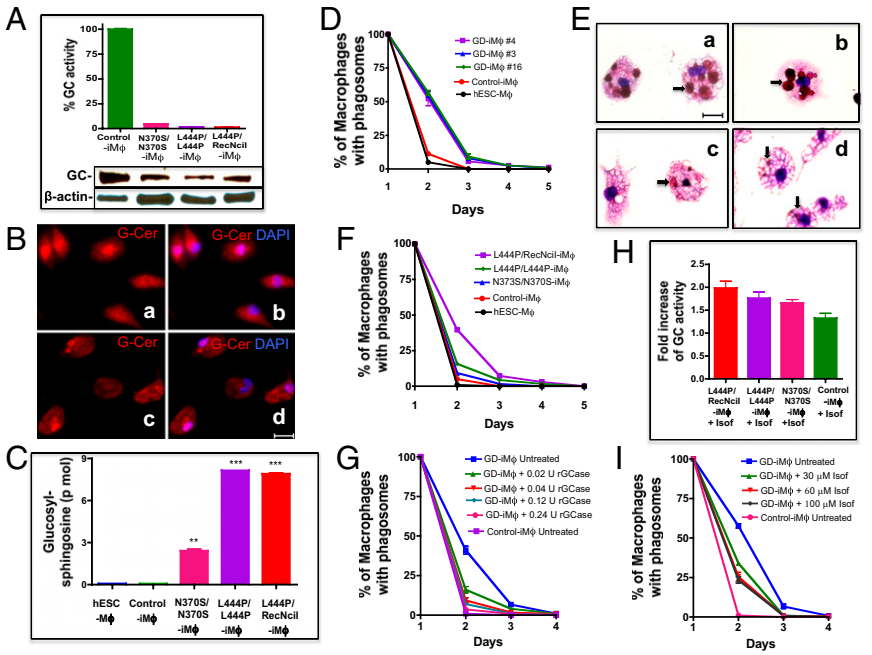

Fig. 3. Phenotype of GD hiPSC-macrophages. (*A*) Low levels of GC enzymatic activity (*Upper*) and GC protein (*Lower*) in N370S/N370S, L444P/L444P, and L444P/Rec*NciI* hiPSC- vs. control hiPSC-macrophages (iMϕ). (*B*) Staining of L444P/Rec*NciI* (*a* and *b*) and control (*c* and *d*) hiPSC-macrophages with rabbit antibodies to GlcCer (G-Cer, red) and nuclear staining with DAPI (blue). (*C*) HPLC-MS/MS analysis showing the level of glucosylsphingosine in H9/hESC-, control hiPSC-, N370S/N370S, L444P/L444P, and L444P/Rec*NciI*-hiPSC-macrophages. (*D*) Kinetics of phagocytosed RBC clearance in different lines of L444P/Rec*NciI* mutant macrophages. H9/hESC- (black), control hiPSC- (red), and three lines of L444P/Rec*NciI* GD hiPSC-macrophages [#3 (blue), #4 (purple), and #16 (green)] were incubated with opsonized RBC, and the time course of RBC clearance was followed. The ordinate represents the percent of GD hiPSC-macrophages containing visible RBC. On day 2, $P < 0.0001$. (*E*) Significant numbers of phagocytosed RBC are still visible 24 h after ingestion by L444P/Rec*NciI* hiPSC-macrophages. L444P/Rec*NciI* hiPSC-macrophages (*a* and *b*) and control hiPSC-macrophages (*c* and *d*) were incubated with opsonized RBC as described above, and cells were stained with May–Grünwald–Giemsa 24 h later. Representative microscopic images are shown. Arrows indicate RBC remnants. (*F*) Comparison of the time courses of RBC clearance in type 1 N370S/N370S (blue), type 2 L444P/Rec*NciI* (purple), and type 3 L444P/L444P (green) macrophages, in control hiPSC- (red), and in H9/hESC-macrophages (black). On day 2, *P* values corresponding to the type 1, 2, and 3 genotypes compared with the controls were $P < 0.008$, $P < 0.0001$, and $P < 0.001$, respectively. (*G*) Phenotypic correction of mutant phenotype by recombinant GC. Untreated control hiPSC-macrophages (purple), untreated L444P/Rec*NciI* hiPSC-macrophages (blue), and L444P/Rec*NciI* hiPSC-macrophages treated with 0.02 (green), 0.04 (red), 0.08 (light blue), and 0.24 (pink) U/mL recombinant GC, as described in *SI Materials and Methods*, were assayed for RBC clearance. On day 2, *P* values for 0.02, 0.04, 0.08, and 0.24 U/mL GC were $P < 0.0015$, $P < 0.005$, $P < 0.0005$, and $P < 0.0001$, respectively. (*H*) Isofagomine treatment increases GC enzyme activity in mutant macrophages. L444P/Rec*NciI*, L444P/L444P, N370S/N370S, and control hiPSC-macrophages were incubated in the presence or absence of 60 μM isofagomine for 5 d; then GC activity was determined. Numbers represent fold-increase of GC activity in treated vs. untreated cells. (*I*) Time course of phagocytosed RBC clearance by GD hiPSC-macrophages in the absence or presence of isofagomine. L444P/Rec*NciI* hiPSC-macrophages were incubated in the absence (blue) or presence of 30 μM (green), 60 μM (red), or 100 μM (black) isofagomine for 5 d and then were assayed for RBC clearance as described in *D*. Untreated H9/hESC macrophages were used as a control (pink). Isofagomine treatment was continued for the duration of the RBC clearance assay. On day 2, *P* values for 30 μM and 60 μM isofagomine were $P < 0.0002$ and $P < 0.0006$, respectively. (Scale bars, 20 μm in *B* and *E*.)

rates of RBC ingestion by GD hiPSC-, control hiPSC-, and hESC-macrophages (Fig. 2*D* and Fig. S3 *E*, *a* and *F*, *a*). Future analysis should clarify the precise steps in the phagocytic cascade that are blocked, and how this blockage relates to the pathophysiology of GD.

Phenotypic Correction of GD hiPSC-Macrophage Defects by Recombinant GC. As shown in Fig. 3*G*, treatment of type 2 L444P/Rec*NciI* hiPSC-macrophages with mannose-exposed recombinant GC restored clearance of phagocytosed RBC in a dose-dependent manner, to almost the same levels as those in control hiPSC-macrophages. Recombinant GC also corrected the defect in RBC clearance in L444P/L444P (type 3) and N370S/N370S (type 1) mutant macrophages (Fig. S6). GC treatment of control hiPSC-macrophages caused only a very slight increase in the rate of RBC clearance. These results suggested that the phenotype we observed was indeed caused by the GC deficiency and, importantly, that the uptake of recombinant GC was able to overcome the deleterious effects of different mutant GC proteins, including the severe L444P and Rec*NciI* mutations in the type 2 hiPSC-macrophages.

Isofagomine Partially Corrects the Abnormal GD hiPSC-Macrophage Phenotype. Isofagomine is a competitive inhibitor of GC that facilitates folding and transport of GC mutants, including the frequent alleles N370S and L444P (23, 24). Isofagomine has been evaluated as a possible therapeutic agent for GD in cell lines, animal models, and clinical trials (24, 25). Isofagomine treatment of types 1, 2, and 3 GD hiPSC-macrophages increased GC enzymatic activity by about 1.7- to 2.0-fold, as compared with 1.3-fold in control cells (Fig. 3*H*). To determine whether this drug would have any effect on RBC clearance by GD hiPSC-macrophages, we incubated L444P/Rec*NciI* GD hiPSC-macrophages with isofagomine for 5 d. After this time, the treated macrophages were incubated with opsonized RBC, and the rate of RBC clearance was followed for 3 d in the presence of isofagomine. As shown in Fig. 3*I*, isofagomine treatment resulted in a partial increase in the rate of clearance of phagocytosed RBC by L444P/Rec*NciI* hiPSC-macrophages. Isofagomine treatment also increased the rates of phagocytosed RBC clearance in L444P/L444P and N370S/N370 hiPSC-macrophages, but it was not as effective as recombinant GC in restoring normal RBC clearance, even in the milder N370S/N370S mutant (Fig. S7*D*). Similar results were obtained regardless of whether isofagomine was added or omitted during the 3-d period following RBC uptake. Taken together, these results reflect the clinical efficacy of enzyme replacement therapy (ERT) and isofagomine, and suggest that GD hiPSC and the functional RBC assay described in this study will be very valuable for evaluating the therapeutic efficacy of new drugs.

Differentiation of GD hiPSC to the Neuronal Lineage. We then investigated whether GD hiPSC could be differentiated to neuronal cell types in vitro. Types 1, 2, and 3 GD hiPSC were differentiated to neuronal cells efficiently; representative results are shown for L444P/Rec*NciI* hiPSC in Fig. 4. Neural tube-like rosettes derived from the neuroepithelial cells expressed markers of neuronal differentiation, including MAP2 and Tuj1. Fig. 4 *A*–*E* shows the characteristic arrangements of the cells in the rosettes, which were positive for the neural progenitor marker SOX2 and the astrocyte marker GFAP (Fig. 4 *D* and *E*). In cultures maintained for over 10–15 d we observed neuronal maturation with establishment of interneuronal connections, and these cells were

positive for neuronal-specific markers including Tuj1, MAP2, and GABA (Fig. 4 *F–H*). These cultures were also positive for dopaminergic neuronal markers such as dopamine β hydroxylase (DβH) and tyrosine hydroxylase (TH) (Fig. 4 *I* and *J*). The rosettes also gave rise to astrocytes and oligodendrocytes, as determined by GFAP and O4 staining, respectively (Fig. 4 *E* and *K*). Importantly, all three types of GD hiPSC-derived neurons had very low GC enzymatic activity (Fig. 4*L*) and accumulated glucosylsphingolipids (Fig. S8).

Discussion

In this study we describe the generation of hiPSC derived from patients with the three clinical subtypes of GD and their proposed use for disease modeling and therapeutic evaluation. The cells used for hiPSC generation were obtained from an adult donor harboring N370S/N370S (type 1), from a 3-y-old donor with type 3 GD carrying L444P/L444P, and from an infant with type 2 GD with heteroallelic L444P/Rec*NciI* mutations. L444P is the second most frequent mutation among patients with GD, and it is often associated with the severe type 2 and 3 forms of GD. The Rec*NciI* allele results from recombination of the *GBA* gene with the *GBA* pseudogene, which harbors an L444P, an A456P, and a silent V460V mutation (26). In type 2 cases, pathological abnormalities are already present in utero, resulting in either fetal mortality or in newborns afflicted by severe visceral and neurological manifestations (4). We have shown that hiPSC-derived cells from all three types of GD have phenotypic abnormalities that increase with the severity of the mutation, and that in every case recombinant GC can reverse these abnormalities.

The most distinguishing histological finding in GD is the presence of Gaucher macrophages in the spleen, liver, and bone marrow, and these cells are believed to be primarily responsible for the visceral, hematologic, and bone pathology in affected individuals (1). GD macrophages are engorged with GlcCer, and GC deficiency also leads to accumulation of glucosylsphingosine, a sphingolipid that is present in very small quantities in normal cells but is highly elevated in tissues of patients who have GD (27). To model the formation of GD macrophages, we carried out directed differentiation of GD hiPSC in the presence of M-CSF. The GD hiPSC-macrophages we obtained had elevated levels of GlcCer and glucosylsphingosine in their resting state. Thus, the level of mutant GC enzyme was insufficient to catabolize glucosylsphingolipids generated by the normal metabolism of the mutant cells, rendering them particularly susceptible to the added digestive burden following erythrophagocytosis. One of the most interesting findings of this study was that GC deficiency resulted in delayed clearance of phagocytosed RBC by GD hiPSC-macrophages. Furthermore, we observed an inverse correlation between the rate of RBC clearance and the severity of the mutation. These observations suggest that the functional assay developed using hiPSC-macrophages may reflect the extent of visceral abnormalities in GD patients, and that GD hiPSC can be very valuable for modeling the molecular and subcellular mechanisms that underlie the pathology of GD. The incomplete digestion of phagocytosed RBC was not secondary to increased uptake of RBC by GD hiPSC-macrophages, because we detected no difference in the rate of erythrophagocytosis between mutant and control macrophages. Rather, the delay in RBC clearance was probably caused by blockage of steps that occur after RBC uptake. Remnants of RBC are frequently observed in Gaucher macrophages isolated from patient bone marrow (17, 18, 21, 22), lending support to the conclusion that the phenotype of GD hiPSC-macrophages that we observed recapitulated that of Gaucher cells.

ERT is the standard of treatment for type 1 GD, and it is also used to alleviate the visceral and hematologic abnormalities in types 2 and 3 GD (28). Cerezyme (imiglucerase; Genzyme), the first enzyme preparation used for ERT, is a recombinant human GC that is modified by glycosidase treatment to facilitate macrophage uptake through mannose receptors. In most patients with type 1 GD, ERT can reduce the visceral and hematologic involvement within 6 mo of the start of regular enzyme infusions (29). Our results showed that incubation of hiPSC-macrophages from all three types of GD with GC restored the clearance of phagocytosed RBC almost to control levels, even in type 2 hiPSC-derived macrophages. Thus, administration of normal GC was able to overcome potential gain-of-function effects of some of the most harmful *GBA* mutations. These observations suggest that it may be possible to identify new therapeutic agents also capable of reversing the deleterious effects of different *GBA* mutations. In future studies with a larger and genotypically diverse GD hiPSC collection, we will examine whether the in vitro response of induced macrophages to recombinant GC correlates with the clinical efficacy of ERT to alleviate visceral manifestations of GD in the corresponding donors.

A number of chaperones and other small molecules that have been tested as potential therapeutic candidates for GD have been

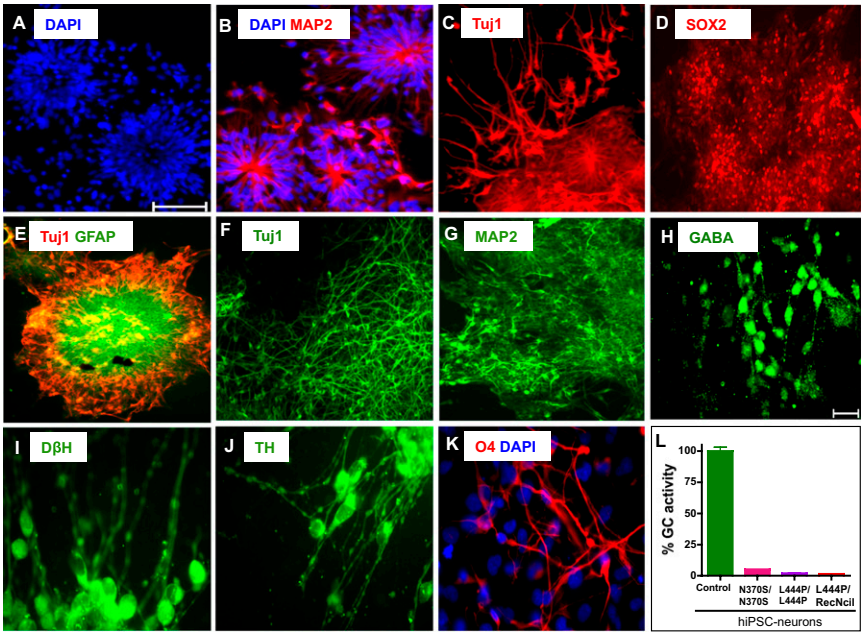

Fig. 4. Differentiation of GD hiPSC to neuronal cells. L444P/Rec*NciI* hiPSC were differentiated to neuronal cells as described in *SI Materials and Methods*, and were stained with antibodies to the indicated markers. (*A–E*) Characterization of neuronal rosette progenitors. (*A*) DAPI (blue). (*B*) MAP2 (red) overlaid with DAPI. (*C*) Tuj1 (red). (*D*) SOX2 (red). (*E*) GFAP (green) overlaid with Tuj1 (red). (*F–K*) Characterization of GD hiPSC neuronal cells extending from rosettes. (*F*) Tuj1 (green). (*G*) MAP2 (green). (*H*) GABA (green). (*I*) DβH (green). (*J*) TH (green). (*K*) O4 (red) overlaid with DAPI. (*L*) Low levels of GC enzymatic activity in N370S/N370S, L444P/L444P, and L444P/Rec*NciI* hiPSC- vs. control hiPSC-neurons. (Scale bars, 100 μm in *A–G*, 20 μm in *H–K*.)

identified in chemical screens using purified GC, followed by validation using human GD cell lines (30, 31). Isofagomine is a competitive inhibitor of GC that facilitates folding and transport of GC mutants, including the frequent N370S and L444P alleles (32, 33), and has been effective in animal models (24, 25). In a 6-mo phase II clinical trial, isofagomine administration increased GC activity in white blood cells in all patients, including homozygous L444P cases, although meaningful clinical improvement was seen in only 1 of 18 patients (24). Isofagomine treatment of GD hiPSC-macrophages resulted in increased GC activity, but this treatment led to only partial restoration of the ability of types 1, 2, and 3 GD hiPSC-macrophages to clear ingested RBC. Thus, in our system, isofagomine was less effective than recombinant GC in correcting the functional defects of GD hiPSC-macrophages harboring different *GBA* mutations, reflecting the clinical experience with these therapeutic agents. Taken together, our results strongly suggest that the functional assay reported in this study may be a very discriminating tool for the assessment of therapeutic efficacy. However, this conclusion needs to be validated with a larger patient population for each clinical subtype.

Impaired lysosomal function in GD neurons is likely to interfere with critical cellular functions such as autophagy, intracellular transport, vesicle fusion, and lysosomal clearance of protein aggregates and organelles targeted for degradation (34, 35). Mutations in *GBA* have been associated with increased risk of Parkinson disease (36), and recent studies using primary cells and GD hiPSC harboring an N370S/84GG genotype (8) showed that dopaminergic neurons exhibited decreased lysosomal protein degradation, accumulation of aggregated α-synuclein, and neurotoxicity (37). In the present study we have shown that GD hiPSC can be efficiently differentiated to neuronal cell types, and that the mutant neurons accumulate glucosylsphingolipids. In future studies, GD hiPSC-neurons will be used for studying the molecular basis of the neuronopathy found in patients with neuronopathic GD.

In summary, we have described the generation of GD hiPSC, their directed differentiation to macrophages and neuronal cells, and have shown their potential to model the functional defects of GD macrophages. GD hiPSC-macrophages recapitulated the lipid storage and impaired RBC clearance phenotype of macrophages infiltrating patient organs (18, 21, 22). In the case of type 2 GD hiPSC-macrophages, this phenotype was striking. We also showed that the functional response of the mutant macrophages to ERT and isofagomine reflected the clinical experience with these therapeutic agents. The generation of GD-hiPSC representative of types 1, 2, and 3 GD and the ability to differentiate them to the affected cell types with high efficiency will help elucidate the mechanisms leading to GD, and will provide a unique platform for drug discovery.

Materials and Methods

Details for the reprogramming of skin fibroblasts from patients with types 1, 2, and 3 GD, harboring N370S/N370S, L444P/Rec*Ncil*, and L444P/L444P mutations in GC, respectively, into hiPSC using the STEMCCA vector, and their characterization are described in *SI Materials and Methods*. The methods for differentiation of hiPSC to macrophages and neurons and their characterization by immunofluorescence analysis and flow cytometry also are described in *SI Materials and Methods*. The GC enzyme assay, analysis of glucosylsphingosine by HPLC-MS/MS, the erythrophagocytosis assay, and treatments with recombinant GC and the chaperone isofagomine are described in *SI Materials and Methods*.

ACKNOWLEDGMENTS. We thank Gustavo Mostoslavsky (Boston University) for providing the STEMCCA vector and Avital Shimanovich and Vivek Bose for expert technical assistance. This work was supported by Grants 2009-MSCRFII-0082-00 (to R.A.F.), 2007-MSCRFE-0110-00 (to R.A.F.), 2011-MSCRF II-0008-00 (to E.T.Z.), and 2007-MSCRF II-0379-00 (to E.T.Z.) from the Maryland Stem Cell Research Fund (MSCRF), Grant 6-FY10-334 (to R.A.F.) from the March of Dimes, and Grants 1U01HL099775 and U01HL100397 (both to E.T.Z.) from the National Institutes of Health. T.S.P. and O.A. are recipients of MSCRF postdoctoral fellowship grants.

1. Beutler E, Grabowski GA (2001) *Gaucher Diseases. The Metabolic and Molecular Bases of Inherited Disease. III* (McGraw-Hill, New York), pp 3635–3668.
2. Messner MC, Cabot MC (2010) Glucosylceramide in humans. *Adv Exp Med Biol* 688 (688):156–164.
3. Jmoudiak M, Futerman AH (2005) Gaucher disease: Pathological mechanisms and modern management. *Br J Haematol* 129(2):178–188.
4. Sidransky E (2004) Gaucher disease: Complexity in a "simple" disorder. *Mol Genet Metab* 83(1-2):6–15.
5. Goker-Alpan O, et al. (2005) Divergent phenotypes in Gaucher disease implicate the role of modifiers. *J Med Genet* 42(6):e37.
6. Takahashi K, Yamanaka S (2006) Induction of pluripotent stem cells from mouse embryonic and adult fibroblast cultures by defined factors. *Cell* 126(4):663–676.
7. Takahashi K, et al. (2007) Induction of pluripotent stem cells from adult human fibroblasts by defined factors. *Cell* 131(5):861–872.
8. Park IH, et al. (2008) Disease-specific induced pluripotent stem cells. *Cell* 134(5):877–886.
9. Yu J, et al. (2007) Induced pluripotent stem cell lines derived from human somatic cells. *Science* 318(5858):1917–1920.
10. Dimos JT, et al. (2008) Induced pluripotent stem cells generated from patients with ALS can be differentiated into motor neurons. *Science* 321(5893):1218–1221.
11. Agarwal S, et al. (2010) Telomere elongation in induced pluripotent stem cells from dyskeratosis congenita patients. *Nature* 464(7286):292–296.
12. Itzhaki I, et al. (2011) Modelling the long QT syndrome with induced pluripotent stem cells. *Nature* 471(7337):225–229.
13. Lahti AL, et al. (2012) Model for long QT syndrome type 2 using human iPS cells demonstrates arrhythmogenic characteristics in cell culture. *Dis Model Mech* 5(2):220–230.
14. Lee G, Studer L (2011) Modelling familial dysautonomia in human induced pluripotent stem cells. *Philos Trans R Soc Lond B Biol Sci* 366(1575):2286–2296.
15. Israel MA, et al. (2012) Probing sporadic and familial Alzheimer's disease using induced pluripotent stem cells. *Nature* 482(7384):216–220.
16. Robinton DA, Daley GQ (2012) The promise of induced pluripotent stem cells in research and therapy. *Nature* 481(7381):295–305.
17. Bitton A, Etzell J, Grenert JP, Wang E (2004) Erythrophagocytosis in Gaucher cells. *Arch Pathol Lab Med* 128(10):1191–1192.
18. Machaczka M, Klimkowska M, Regenthal S, Hägglund H (2011) Gaucher disease with foamy transformed macrophages and erythrophagocytic activity. *J Inherit Metab Dis* 34(1):233–235.
19. Polumuri SK, Toshchakov VY, Vogel SN (2007) Role of phosphatidylinositol-3 kinase in transcriptional regulation of TLR-induced IL-12 and IL-10 by Fc gamma receptor ligation in murine macrophages. *J Immunol* 179(1):236–246.
20. Naito M, Takahashi K, Hojo H (1988) An ultrastructural and experimental study on the development of tubular structures in the lysosomes of Gaucher cells. *Lab Invest* 58(5): 590–598.
21. Lee RE, Balcerzak SP, Westerman MP (1967) Gaucher's disease. A morphologic study and measurements of iron metabolism. *Am J Med* 42(6):891–898.
22. Hibbs RG, Ferrans VJ, Cipriano PR, Tardiff KJ (1970) A histochemical and electron microscopic study of Gaucher cells. *Arch Pathol* 89(2):137–153.
23. Kornhaber GJ, et al. (2008) Isofagomine induced stabilization of glucocerebrosidase. *ChemBioChem* 9(16):2643–2649.
24. Khanna R, et al. (2010) The pharmacological chaperone isofagomine increases the activity of the Gaucher disease L444P mutant form of beta-glucosidase. *FEBS J* 277(7):1618–1638.
25. Sun Y, et al. (2012) Ex vivo and in vivo effects of isofagomine on acid β-glucosidase variants and substrate levels in Gaucher disease. *J Biol Chem* 287(6):4275–4287.
26. Hruska KS, LaMarca ME, Scott CR, Sidransky E (2008) Gaucher disease: Mutation and polymorphism spectrum in the glucocerebrosidase gene (GBA). *Hum Mutat* 29(5):567–583.
27. Orvisky E, et al. (2002) Glucosylsphingosine accumulation in tissues from patients with Gaucher disease: Correlation with phenotype and genotype. *Mol Genet Metab* 76(4): 262–270.
28. Brady RO (2006) Enzyme replacement for lysosomal diseases. *Annu Rev Med* 57:283–296.
29. Goker-Alpan O (2011) Therapeutic approaches to bone pathology in Gaucher disease: Past, present and future. *Mol Genet Metab* 104(4):438–447.
30. Yu Z, Sawkar AR, Kelly JW (2007) Pharmacologic chaperoning as a strategy to treat Gaucher disease. *FEBS J* 274(19):4944–4950.
31. Zheng W, et al. (2007) Three classes of glucocerebrosidase inhibitors identified by quantitative high-throughput screening are chaperone leads for Gaucher disease. *Proc Natl Acad Sci USA* 104(32):13192–13197.
32. Shen JS, Edwards NJ, Hong YB, Murray GJ (2008) Isofagomine increases lysosomal delivery of exogenous glucocerebrosidase. *Biochem Biophys Res Commun* 369(4):1071–1075.
33. Steet RA, et al. (2006) The iminosugar isofagomine increases the activity of N370S mutant acid beta-glucosidase in Gaucher fibroblasts by several mechanisms. *Proc Natl Acad Sci USA* 103(37):13813–13818.
34. Settembre C, et al. (2008) A block of autophagy in lysosomal storage disorders. *Hum Mol Genet* 17(1):119–129.
35. Sun Y, Grabowski GA (2010) Impaired autophagosomes and lysosomes in neuronopathic Gaucher disease. *Autophagy* 6(5):648–649.
36. Goker-Alpan O, et al. (2008) The spectrum of parkinsonian manifestations associated with glucocerebrosidase mutations. *Arch Neurol* 65(10):1353–1357.
37. Mazzulli JR, et al. (2011) Gaucher disease glucocerebrosidase and α-synuclein form a bidirectional pathogenic loop in synucleinopathies. *Cell* 146(1):37–52.